NANO LETTERS

LETTER

pubs.acs.org/NanoLett

Porous PVDF As Effective Sonic Wave Driven Nanogenerators

SeungNam Cha,[†,§] Seong Min Kim,[†,§] HyunJin Kim,[†] JiYeon Ku,[†] Jung Inn Sohn,[†] Young Jun Park,[†] Byong Gwon Song,[†] Myoung Hoon Jung,[†] Eun Kyung Lee,[†] Byoung Lyong Choi,[†] Jong Jin Park,[†] Zhong Lin Wang,[*,‡] Jong Min Kim,[*,†] and Kinam Kim[†]

[†]Frontier Research Laboratory, Samsung Advanced Institute of Technology, Yongin, 449-712, Republic of Korea

[‡]School of Materials Science and Engineering, Georgia Institute of Technology, Atlanta, Georgia 30332, United States

Supporting Information

ABSTRACT: Piezomaterials are known to display enhanced energy conversion efficiency at nanoscale due to geometrical effect and improved mechanical properties. Although piezoelectric nanowires have been the most widely and dominantly researched structure for this application, there only exist a limited number of piezomaterials that can be easily manufactured into nanowires, thus, developing effective and reliable means of preparing nanostructures from a wide variety of piezomaterials is essential for the advancement of self-powered nanotechnology. In this study, we present nanoporous arrays of polyvinylidene fluoride (PVDF), fabricated by a lithography-free, template-assisted preparation method, as an effective alternative to nanowires for robust piezoelectric nanogenerators. We further demonstrate that our porous PVDF nanogenerators produce the rectified power density of 0.17 mW/cm^3 with the piezoelectric potential and the piezoelectric current enhanced to be 5.2 times and 6 times those from bulk PVDF film nanogenerators under the same sonic-input.

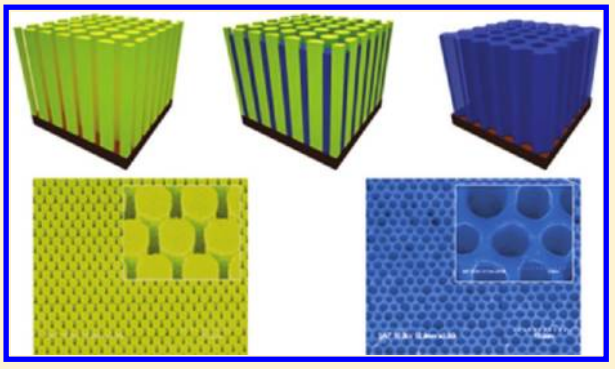

KEYWORDS: Nanogenerator, nanoporous structure, piezomaterials, and energy harvesting

Energy is a vital factor in making life sustainable. Although fossil fuels are the main source of the current energy consumption, their adverse effects on the environment are catalyzing studies of new sources of clean energy generation. Piezoelectric energy generator, harvesting electrical energy from various mechanical sources such as mechanical vibration,[1] ultrasonic wave,[2] and even sound noise,[3] is one of the promising green methods of energy generation. Advances in nanotechnology have also stimulated studies of the nanoscale manipulation of piezoelectric materials in energy-related applications since Wang et al. introduced nanowire-based piezoelectric generation in 2006.[4] Nanostructure-based piezo-energy harvesting is especially appealing due to the apparent strain confinement effect in nanostructures as well as the huge strain that can be tolerated by nanostructures. Stress applied mechanically along an axis causes strain not only in that axial direction but also in orthogonal directions.[5] If the structural size in the orthogonal directions is reduced, strain becomes more effectively confined to the axial direction. In piezoelectric materials, such geometric strain confinement leads to better aligned dipoles and an increased piezoelectric potential. Energy generators made with nanowire arrays, in fact, have been demonstrated to display promising performance,[4] and their small size also broadens the range of applications in which mechanical energy can be recycled and used as the energy source, especially for powering mobile and wireless electronics.

Despite considerable research efforts on the nanogenerators in recent years, the basic scheme for fabricating the device has changed little. Quasi one-dimensional structures such as nanowires, nanofibers, and nanoribbons have been almost exclusively considered as the piezoelectric active component. However, those fabrication methods for nanostructures are available only for a limited number of piezoelectric materials such as zinc oxide (ZnO),[4] gallium nitride (GaN),[6] and lead zirconate titanate (PZT).[1] As a result, not only has the scope of the research been restricted to manipulating device dimensions or exploring possible applications, but more importantly, a large number of piezoelectric materials with a much better efficiency have been disqualified due to the lack of fabrication method for nanostructuring. In this paper, we explore porous piezoelectric nanostructures as an alternative and general method to piezoelectric nanowires to overcome the limits and demonstrate a new template-assisted approach by which porous piezoelectric nanogenerators (PNGs) can be fabricated from a variety of high-efficient piezomaterials without complicated growth or lithographic techniques to make array structures. The superior performance of the structure for energy harvesting is demonstrated.

Received: June 30, 2011
Revised: October 24, 2011

dx.doi.org/10.1021/nl202208n | *Nano Lett.* XXXX, XXX, 000–000

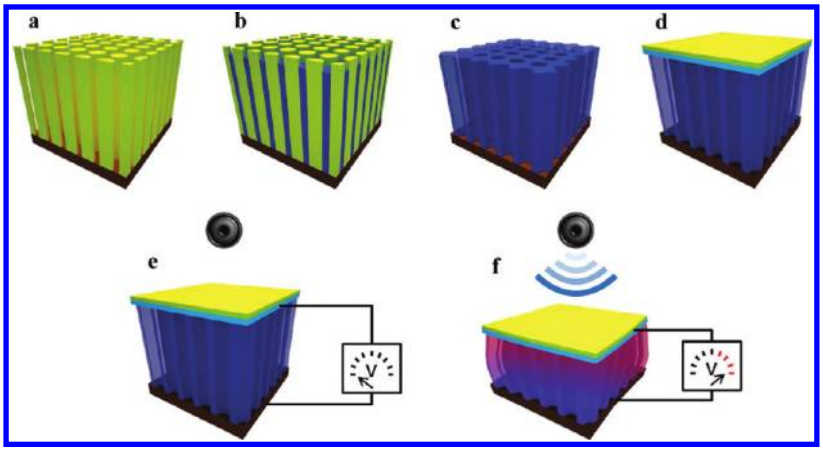

Figure 1. Schematic depiction of the fabrication process and device measurement for nanoporous structures: (a) vertically grown nanowire array, (b) application of piezoelectric material onto the template, (c) nanowire template etching/thermal annealing, (d) assembling top electrode (Au-coated PET substrate) and electrical polling, (e) measurement setup for sonic wave driven piezoelectric nanogenerator, and (f) piezoelectric potential of PNGs generated by the sonic wave.

Our approach begins from the idea that the strain confinement effect results in the enhanced piezoelectric potential in the piezoelectric nanowires that should also hold in the case of porous piezoelectric nanostructures. Figure 1 shows a schematic drawing of our fabrication process for preparing narrow nanoporous arrays of piezoelectric materials. In this approach, a nanowire array is used as the basic template. Vertically aligned carbon nanotubes or ZnO nanowires are good candidates as there are well-established growth techniques. After a target piezomaterial is deposited atop the template filling the space between nanowires, the template is removed by etching, and annealing process follows if necessary. In order to align the electric dipoles within the exposed porous piezoelectric nanostructure, polling is carried out by applying an electric field between the top and the bottom electrodes. Using the resulting porous structures, nanogenerators are devised via previously described method, and their energy harvesting performance is examined using sonic wave as the input source.[3] In principle, our template-assisted preparation method can be applied to any combination of nanowires and piezomaterials with appropriate etching selectivity that ensures an easy removal of the nanowire template, and it is particularly powerful for those polymeric piezomaterials with high energy conversion efficiency.

Next, we demonstrate a successful application of our method in fabricating porous nanostructures of the polymeric piezomaterial, PVDF (polyvinylidene fluoride). PVDF has a high piezoelectric coefficient (d_{33} = −32.5 pC/N), and its flexibility and transparency present additional advantages in many piezoelectric applications. However, it has remained a great challenge to fabricate nanostructures using such a material. Figure 2a shows a porous PVDF nanostructure using a ZnO nanowire template (the spacing between the pores is estimated to be ∼100 nm). The nanowires were etched away to obtain the final nanoporous structure. Inset of Figure 2a shows a SEM image before removing ZnO nanowires. The integrated porous PVDF nanogenerators (porous piezoelectric nanogenerator) have the volume of 1 cm × 1 cm × 5 μm. Their piezoelectric characteristics were measured from peak-to-peak piezoelectric potential (open circuit voltage, 2.6 V) and current (short circuit current, 0.6 μA) under the sonic input (100 dB, 100 Hz) (Figure 2b). To identify true signals from PNGs, a switching polarity test was done, meaning that a change in electrical connection (forward ↔ reverse) resulted in a reversal in the measured output. We have shown identical characteristics of the switching polarity by both of physical impulses (Figure 2c) and sonic waves (Figure 2d). Also, in order to understand the enhanced piezoelectric potential in the PNGs, systematic modeling and experiment was carried out.

As in the case of nanowires,[7] observed enhancement in piezoelectric potential can be explained by geometrical strain confinement effect. The smaller the interpore distance is, the more effective the strain is confined. The interpore distance is defined as the shortest wall-to-wall distance between two neighboring pores. We chose PVDF as the representative model piezomaterial and carried out a systematic numerical simulation to confirm the interpore distance dependency of the piezoelectric potential. Using the finite element method (FEM, COMSOL), the piezoelectric potential of a fully coupled electromechanical system was calculated from the piezoelectric coupled equations.[5] PVDF was assumed to be a dielectric polymer, and its elastic and piezoelectric constants were taken from ref 8. Figure 3a shows the calculated piezoelectric potential under the same stress along the z-axis (polling direction) as a function of interpore distance. The porous structure are constructed by placing hexagonally arranged pores which vertically penetrate the 23.3 μm × 26.9 μm × 5 μm (height) slab of PVDF. The pores are modeled as hexagonal cylinders with the diameter (the longest diagonal of the hexagon) of 2 μm (inset of Figure 3a). The bottom of the PVDF structure was affixed to a substrate and electrically grounded. A constant external stress Tz (= -2.1×10^5 Pa) is exerted along the z-axis from the top of the structure, and the induced piezoelectric potential is calculated along the vertical axis at the center of the triangle formed by three neighboring pores located near the center of model. As expected, the piezoelectric potential is found to increase with decreasing interpore distance. This is because the structure with a smaller interpore distance restricts stress relaxation in the $x-y$ plane more effectively, which consequently increases the strain in the z-direction.

To further understand the enhanced piezoelectric potentials upon geometrical changes, we examine the effective piezoelectric coefficient[5,7,9] because it is directly associated with piezoelectric potential. Note that the axis of input stress and the polling axis are the same (z-axis) in our PVDF system, thus the relevant is d_{33}^{eff}

dx.doi.org/10.1021/nl202208n |*Nano Lett.* XXXX, XXX, 000–000

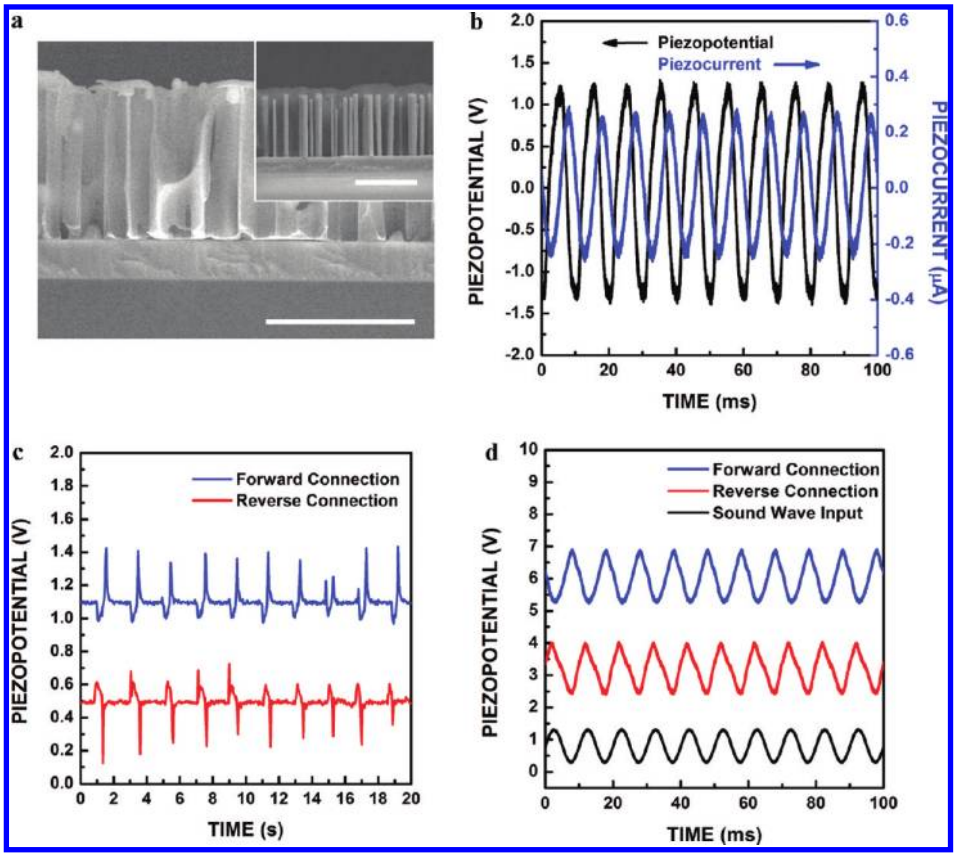

Figure 2. (a) Cross section SEM images. Scale bars are 5 μm. A porous PVDF nanostructure using a ZnO nanowire template (inset shows a SEM image before removing ZnO nanowires). (b) Piezoelectric potential/current obtained from the porous PVDF nanostructures at 100 dB and 100 Hz sound input power. (c) Output polarity resulted from physical impulse on the PNGs is changed with forward or reverse connection. (d) Output polarity caused by the sonic waves is also changed with forward or reverse connection.

defined as $(\partial D_3/\partial T_3)$, where E is the electric field, D is the electric displacement, and T is the stress. In view of its 2 mm symmetry,[10] d_{33}^{eff} for the porous PVDF nanostructure can be expressed as follow

$$d_{33}^{\text{eff}} = d_{33} + \left\{ \left(d_{31} - \frac{d_{32} s_{12}^{\text{E}}}{s_{22}^{\text{E}}} \right) \left(\frac{\left(\frac{s_{12}^{\text{E}}}{s_{11}^{\text{E}}} \left(\frac{s_{23}^{\text{E}} + k_2}{s_{22}^{\text{E}}} \right) - \frac{s_{13}^{\text{E}} + k_1}{s_{11}^{\text{E}}} \right)}{\left(1 - \frac{(s_{12}^{\text{E}})^2}{s_{22}^{\text{E}} s_{11}^{\text{E}}} \right)} \right) - d_{32} \left(\frac{s_{23}^{\text{E}} + k_2}{s_{22}^{\text{E}}} \right) \right\} \quad (1)$$

where s_{ij} is the elastic compliance and k_1 and k_2 are the proportionality factors in the x and y direction (see Supporting Information for more details).

As shown in Figure 3b, d_{33}^{eff} approaches the value of d_{33} (= −32.5 pC/N) at a shorter distance away from the substrate as the interpore distance decreases. Here, note that d_{33}^{eff} depends on z-coordinate because k_1 and k_2 are functions of stress (refer to eq S9 in Supporting Information), and these stress terms have variations along the z-axis in our system where the bottom side of the nanoporous structure is clamped to the substrate. The piezoelectric potential can be calculated by integrating d_{33}^{eff} as well as the stress terms (T_1, T_2, and T_3) across the height of the structure (eq S12 in Supporting Information), which essentially is the area bounded by each of the plotted graphs within the appropriate z range (0−5 μm) in Figure 3b (see Supporting Information eqs S1−S12). Therefore, faster saturation of d_{33}^{eff} to d_{33} observed for smaller interpore distances represents greater enhancement in piezoelectric potential, and this behavior is also in agreement with the previous calculation showing interpore distance dependent enhancement in piezoelectric potentials (Figure 3a). In fact, this geometrical effect on the piezoelectric potential change is apparent in eq 1. The second term in eq 1 describes the strain relaxation in the direction orthogonal to the input stress. Consequently, if the strain is effectively confined, as in the case of smaller interpore distance, the second term becomes smaller and tends to zero, such that d_{33}^{eff} is approaching to d_{33}. Therefore, reduction in the interpore distance of the nanoporous structures should result in the enhanced piezoelectric potential.

The effect of interpore distance on the piezoelectric potential in porous PVDF was also examined experimentally. For a systematic investigation, we adopted conventional Si etching techniques to prepare Si pillar templates with interpillar distances ranging from 300 to 5000 nm. Figure 3c1−c4 shows the top views of SEM images of Si pillar templates with interpore distances 300, 500, 1000, and 5000 nm respectively and the tilted image of the Si pillar templates (Figure 3c5). The tilted SEM image of the PVDF-filled template (Figure 3c6) and the cross sectional view (Figure 3c7) with a zoomed in SEM picture of c6 (Figure 3c8) were shown. The tilted SEM images of the

dx.doi.org/10.1021/nl202208n |*Nano Lett.* XXXX, XXX, 000–000

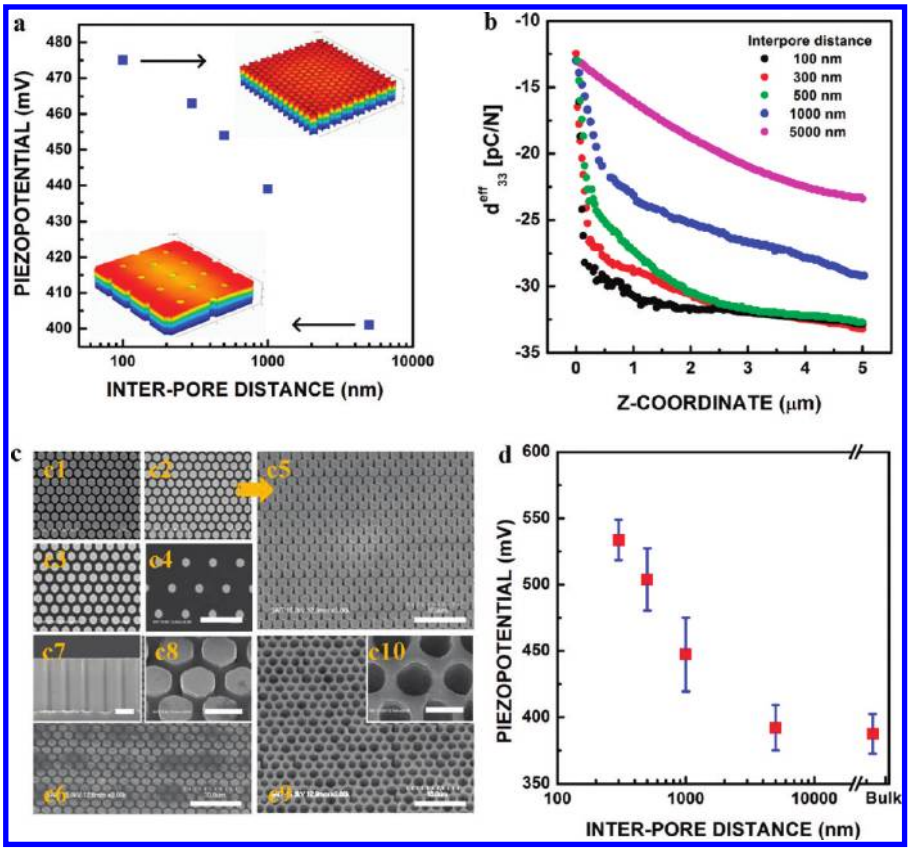

Figure 3. (a) Piezoelectric potentials calculated near the center of porous PVDF nanostructures as a function of interpore distance (100−5000 nm). Insets show the different interpore distance structures used for the FEM calculations (100 and 5000 nm interpore distance structures); red color indicates positive potential, blue indicates the ground potential. (b) Effective piezoelectric coefficients, d_{33}^{eff} for porous PVDF nanostructures (interpore distance ranging from 100 to 5000 nm) along the central axis. (c1−c4) Top views of SEM images of Si pillar templates with interpore distances 300, 500, 1000, and 5000 nm, respectively (scale bar: 10 μm). (c5) Tilted SEM image of Si pillar template with the interpore distance of 500 nm (scale bar: 10 μm). (c6) Tilted SEM images of PVDF-filled templates (scale bars are 10 μm). (c7) Cross sectional SEM image of PVDF-filled Si template (scale bar: 2 μm). (c8) Zoomed-in SEM image of c6 (scale bar: 2 μm). (c9) Tilted SEM image of a Si-etched template after PVDF filling (scale bar: 10 μm). (c10) Zoomed-in SEM image of c9 (scale bar: 2 μm). (d) Piezoelectric output voltages acquired from sonic wave driven PNG. Each point is taken from the peak-to-peak AC output voltage.

top surface of the plasma etched PVDF (nanoporous structure) was shown in Figure 3c9 (inset shows a zoomed-in SEM picture of Figure 3c9: Figure 3c10). The input sound power provides the mechanical energy to be converted into electricity, and it was adjusted from 88.9 to 100 dB at 100 Hz to ensure the same external stress on the PNGs of varying porous and surface areas (Supporting Information Table S1). Alternating piezoelectric potential generated as a result of the sinusoidal input wave[3] is taken to be the peak-to-peak AC output voltage. Measurements were taken from five different devices for each interpore distance. As shown in Figure 3d, the piezoelectric potential increases as the interpore distance decreases, which is in agreement with our calculation. Enhancement in the piezoelectric potential becomes more significant for interpore distances smaller than 1 μm, which we conjecture to be the size at which the strain/stress and the induced polarization become effectively confined along the z-axis. The discrepancy between the simulation results and the experimental measurements is found to be within the error bar range (Figure 3d). The trend observed in our experiment matches that from the numerical simulation well; together they confirm that piezoelectric potential is enhanced in the nanoporous structures as a result of the geometrical strain confinement effect.

Enhanced piezoelectricity in the porous structures can be translated into more efficient piezoelectric nanodevices. In order to demonstrate the potential use of porous piezoelectric systems, the porous PVDF nanostructure prepared via our ZnO nanowire template-assisted method was employed to construct a PNG. With the input sonic power of 100 dB at 100 Hz, the PNG shows a clear enhancement in peak-to-peak piezoelectric potentials (open circuit voltages)/piezoelectric currents (short circuit currents) with the output of 2.6 V/0.6 μA, which is over 5.2 times (piezoelectric potential)/6 times (piezoelectric current) that from the bulk film system (0.5 V/0.1 μA), respectively, under the same force as shown in Figure 4a,b. This clearly indicates that our method in fact effectively enhances piezoelectricity. When the PNGs drive devices, the rectified output power, in general, is important. The charging feature of the capacitor via rectifier was shown in Figure 4c. The output voltage was measured between point A and B with two serially connected capacitors (1 μF each) with all switches turned off as shown in Figure 4d. The voltage of the capacitors was reached to 1.85 V at 10 s, which suggests the output power of 0.17 mW/cm^3 for our PVDF PNG within the charging circuit. In order to operate a light emitting diode (LED), the capacitors were replaced by those with the capacitance of 100 μF, and a voltage doubling

dx.doi.org/10.1021/nl202208n |*Nano Lett.* XXXX, XXX, 000–000

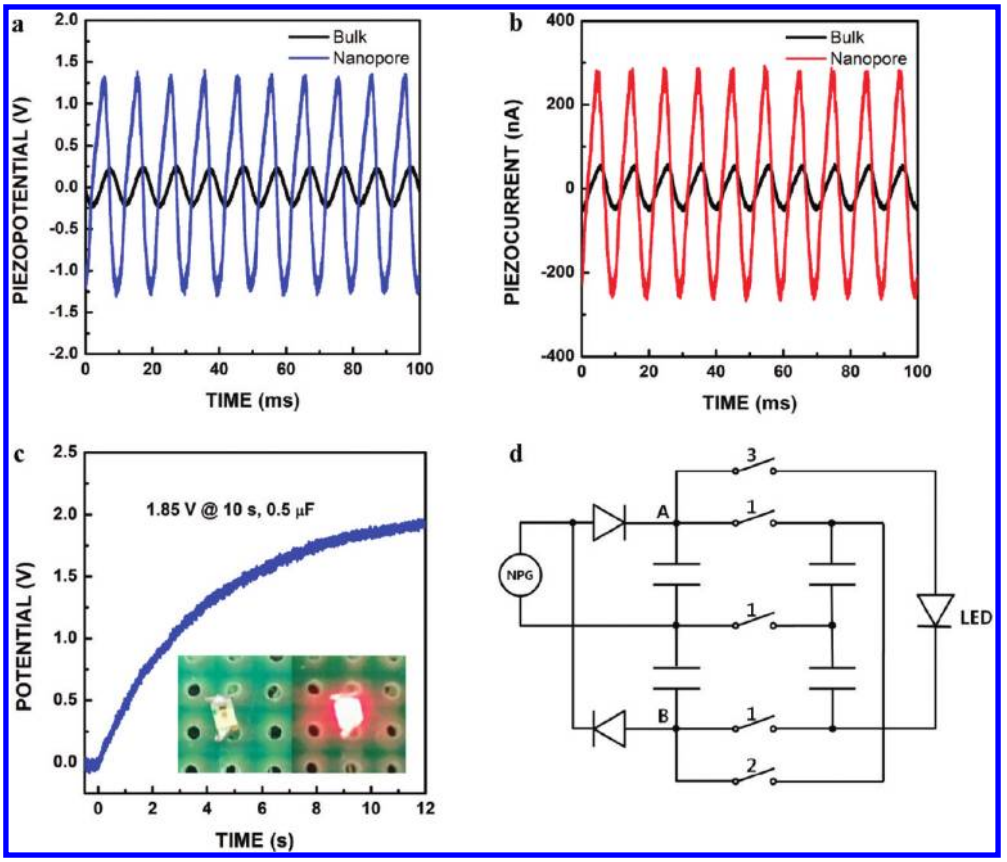

Figure 4. (a) Piezoelectric potential and (b) piezoelectric currents from the porous PVDF and bulk structure under the same force. (c) Voltage across a storage capacitor when being charged by the porous PVDF piezoelectric nanogenerator (inset shows snapshots of the commercial LED before and at the moment of being powered by the stored charges). (d) Schematic design diagram of the rectifying circuit and charge storage devices.

circuit was implemented (Figure 4d), which increased the output voltage to 3.7 V.[11,12] The sonic wave driven PNG charges the capacitors with only the switches numbered 1 turned on; then when the switches numbered 2 and 3 are turned on with the switches numbered 1 turned off, capacitors are discharged to power the LED. In the inset in Figure 4c, we show the successfully powered LED device, and this demonstrates the potential use of the porous piezoelectric nanogenerator in applications such as self-powered sensors and wireless health care systems. In addition, we note that compared to previously reported piezoelectric nanogenerators,[4,11] our PNGs can generate continuous energy even with a very weak input power source as in the case of sonic waves.

Piezoelectric energy generation is a promising energy-harvesting method for powering micro/nanoelectronics. This field has experienced a rapid development with the introduction of nanotechnology. In this work, we have introduced a novel template-assisted fabrication method for porous piezoelectric nanostructures, which allows a broad range of piezomaterials to be made into effective nanoporous structures for high efficient piezoelectric energy generation. We have fabricated porous PVDF structures using this method and demonstrated, both computationally and experimentally, that piezoelectric potential is indeed enhanced in such structures as a result of the geometrical strain confinement. Our approach can be especially powerful when adapted to the large number of piezomaterials with high piezoelectric efficiency such as PVDF. We have additionally demonstrated that the PVDF PNGs present a promising potential for commercial applications in areas such as self-powered sensor networks and wireless healthcare. We expect that our nanopore fabrication method will catalyze further research in diverse piezoelectric materials and their applications at the nanoscale.

Methods. *Fabrication of Nanoporous Structure.* Two types of template were used to make the nanoporous structure. Si pillars were fabricated by a conventional semiconductor process, photo lithography, and dry etching. The other template comprises vertically aligned, hydrothermally synthesized ZnO (Zinc Oxide) nanowires on Si substrate. The nanowires were synthesized by a hydrothermal method. Polymer piezomaterial, PVDF in methyl ethyl ketone (MEK), was coated on the Si pillar or nanowire template after self-assembled monolayer (SAM) treatment using Nafion (0.5 wt % in ethanol) to promote wetting properties of the PVDF solution. We used a two-step coating process to control and obtain the PVDF film thickness of 5−6 μm, and the solution viscosity was adjusted such that the weight percentage of PVDF was in the range of 1.5 to 10%. First, the templates were dipped in 1.5% solution and then carefully sonicated at low power. This step ensures the removal of possible air bubbles or voids near or on the pillar surface. Second, the templates were spin-coated for 30 s at 1500 rpm. The concentrations of PVDF solution were designed according to the interpillar distance of the templates. ZnO NWs and Si pillar templates with interpillar distance having 300 and 500 nm were coated by 4% solution. The 7 and the 10% solution were coated on 1000 and 5000 nm interpillar templates, respectively. A thermal annealing (2 h at 80 °C and 2 h at 130 °C in air) was carried out to form β phase

dx.doi.org/10.1021/nl202208n |*Nano Lett.* XXXX, XXX, 000–000

dominant PVDF.[13−15] A dry etching was performed to expose the top portion of the nanowires, which is covered with PVDF, and to adjust the final film thickness at 5 μm. PVDF was etched by reactive ion etcher (RIE, Nextral) with mixed gas plasma (CF_4 20% + O_2 80%, power 500 W, pressure 100 mTorr). The etching rate was estimated as 10 nm/s. The nanowire/pillar templates were removed in etching solution (10% H_3PO_4 in ethanol for ZnO nanowire etching, 20 wt % KOH in DI water in the case of Si pillar etching). The resulting porous nanostructure was covered with Au-coated polyethylene terephthalate (PET) substrate as the top electrode. The electrical polling process was carried out by applying an electric field between the top electrode and the Si substrate as bottom electrode. An electric field of 60 V/μm was applied for 1 h.[13−15]

■ ASSOCIATED CONTENT

Supporting Information. Additional calculations and table. This material is available free of charge via the Internet at http://pubs.acs.org.

■ AUTHOR INFORMATION

Corresponding Author

*E-mail: (Z.L.W.) zhong.wang@mse.gatech.edu; (J.M.K.) jongkim@samsung.com.

Author Contributions

§These authors contributed equally to the work.

■ ACKNOWLEDGMENT

This work was supported by Global Frontier Research Center for Advanced Soft Electronics.

■ REFERENCES

(1) Xu, S.; et al. Self-powered nanowire devices. *Nat. Nanotechnol.* **2010**, *5*, 366–373.

(2) Wang, X.; et al. Direct-Current Nanogenerator Driven by Ultrasonic Waves. *Science* **2007**, *316*, 102–105.

(3) Cha, S. N.; et al. Sound-Driven Piezoelectric Nanowire-Based Nanogenerators. *Adv. Mater.* **2010**, *22*, 4726–4730.

(4) Wang, Z. L.; et al. Piezoelectric Nanogenerators Based on Zinc Oxide Nanowire Arrays. *Science* **2006**, *312*, 242–246.

(5) Lefki, K.; et al. Measurement of Piezoelectric Coefficients of Ferroelectric Thin Films. *J. Appl. Phys.* **1994**, *76*, 1764–1767.

(6) Zhao, M. H.; et al. Piezoelectric Characterization of Individual Zinc Oxode Nanobelt Probed by Piezoresponse Force Microscope. *Nano Lett.* **2004**, *4*, 587–590.

(7) Huang, C. T.; et al. GaN nanowire arrays for high-output nanogenerators. *J. Am. Chem. Soc.* **2010**, *132*, 4766–4771.

(8) Tarn, J. Q.; et al. Saint-Venant end effects in multilayered piezoelectric laminates. *Int. J. Solids Struct.* **2002**, *39*, 4979–4998.

(9) Standards Committee of the IEEE Ultrasonics, Ferroelectrics, and Frequency Control Society, Part 2, Chapter 2.1−2.6. *IEEE Standard on Piezoelectricity*; The Institute of Electrical and Electronics Engineers, Inc.: New York; 1988.

(10) Mateu, L.; et al. Optimum Piezoelectric Bending Beam Structures for Energy Harvesting using Shoe Inserts. *J. Intell. Mater. Syst. Struct.* **2005**, *10*, 835–845.

(11) Xu, S.; et al. Piezoelectric-nanowire-enabled power source for driving wireless microelectonics. *Nat. Commun.* **2010**, *1:93*, 1–4.

(12) Zhu, G.; et al. Flexible high-output nanogenerator based on lateral ZnO nanowire array. *Nano Lett.* **2010**, *10*, 3151–3155.

(13) Vinogradova, A. M.; et al. Dynamic response of the piezoelectric polymer PVDF. *Int. J. Appl. Electromagn. Mech.* **2005**, *22*, 39–51.

(14) Nalwa, H. S. *Ferroelectric polymer*; Marcel Dekker, Inc.: New York, 1995; Part I, Chapters 2−3.

(15) Kang, S. J.;Spin cast ferroelectric beta poly(vinylidene fluoride) thin films via rapid Thermal annealing. *Appl. Phys. Lett.* **2008**, *92* 012921.